Supplementary Information: Enhancing the Electron Pair Approximation with Measurements on Trapped Ion Quantum Computers

Luning Zhao,[1,*] Qingfeng Wang,[2] Joshua Goings,[1] Kyujin Shin,[3,†] Woomin Kyoung,[3] Seunghyo Noh,[3] Young Min Rhee,[4] and Kyungmin Kim[4]

[1]*IonQ Inc, College Park, MD, 20740, USA*
[2]*Chemical Physics Program and Institute for Physical Science and Technology, University of Maryland, College Park, MD, 20742, USA*
[3]*Materials Research & Engineering Center, Advanced Vehicle Platform Division, Hyundai Motor Company, Uiwang 16082, Republic of Korea*
[4]*Department of Chemistry, KAIST, Daejeon, 34141, Republic of Korea*

(Dated: July 17, 2024)

Supplementary Note 1. COMPUTATIONAL DETAILS

The oo-upCCD circuits are implemented in the Qiskit software platform,[1] and all the simulator results are obtained from the statevector simulator provided by Qiskit. The full configuration interaction (FCI) and the complete active space configuration interaction (CASCI) results were obtained from PySCF[2] package. The Li, O, C, and N 1*s* orbitals are frozen at the restricted Hartree-Fock (RHF) level. For Br and I atoms, all the non-valence orbitals are frozen at the RHF level. The oo-upCCD circuit parameter optimization is performed with the L-BFGS optimization technique. All the calculations are performed using the minimal STO-3G basis. Error bars on the potential energy surface plots represent $\pm$ one standard error as a result of finite sampling. The molecular geometries along the reaction path for CH_2OH^+ decomposition were taken from intrinsic reaction coordinate calculation[3]. The molecular structures along the minimum energy path of S_N2 reaction of $CH_3I + Br^-$ were obtained using the nudged elastic band method[4–6].

Supplementary Note 2. CONSTRUCTION OF 4RDM

In the implementation of the pair-VQE, the Hamiltonian is written as

$$\begin{aligned} H = &\sum_{pq} g_{pq} \left(a^\dagger_{p\alpha} a_{q\alpha} + a^\dagger_{p\beta} a_{q\beta} \right) \\ &+ \sum_{pqrs} (pq|rs) \left(\frac{1}{2} a^\dagger_{p\alpha} a_{q\alpha} a^\dagger_{r\alpha} a_{s\alpha} + \frac{1}{2} a^\dagger_{p\beta} a_{q\beta} a^\dagger_{r\beta} a_{s\beta} \right) \\ &+ \sum_{pqrs} (pq|rs) a^\dagger_{p\alpha} a_{q\alpha} a^\dagger_{r\beta} a_{s\beta} \end{aligned} \tag{1}$$

in which g is the modified one-electron integrals

$$g_{pq} = h_{pq} - \frac{1}{2} \sum_r (pr|rq) \tag{2}$$

and $(pq|rs)$ is the usual two-electron coulomb integrals in $(11|22)$ order.

Therefore, for 4-RDMs, there are three different categories.

$$\begin{aligned} &\left\langle \Psi^{(0)} | a^\dagger_u a_v a^\dagger_x a_y a^\dagger_{p\alpha} a_{q\alpha} a^\dagger_{r\alpha} a_{s\alpha} | \Psi^{(0)} \right\rangle \\ &\left\langle \Psi^{(0)} | a^\dagger_u a_v a^\dagger_x a_y a^\dagger_{p\beta} a_{q\beta} a^\dagger_{r\beta} a_{s\beta} | \Psi^{(0)} \right\rangle \\ &\left\langle \Psi^{(0)} | a^\dagger_u a_v a^\dagger_x a_y a^\dagger_{p\alpha} a_{q\alpha} a^\dagger_{r\beta} a_{s\beta} | \Psi^{(0)} \right\rangle \end{aligned} \tag{3}$$

* zhao@ionq.co

† shinkj@hyundai.com

For each category, there are three sub-categories, which corresponds to $\alpha\alpha$, $\beta\beta$, and $\alpha\beta$ excitations. For example,

$$\begin{aligned}
&\left\langle \Psi^{(0)} | a^\dagger_{u\alpha} a_{v\alpha} a^\dagger_{x\alpha} a_{y\alpha} a^\dagger_{p\alpha} a_{q\alpha} a^\dagger_{r\alpha} a_{s\alpha} | \Psi^{(0)} \right\rangle (x<u, y<v, u\neq v, x\neq y, u\neq y, v\neq x) \\
&\left\langle \Psi^{(0)} | a^\dagger_{u\beta} a_{v\beta} a^\dagger_{x\beta} a_{y\beta} a^\dagger_{p\alpha} a_{q\alpha} a^\dagger_{r\alpha} a_{s\alpha} | \Psi^{(0)} \right\rangle (x<u, y<v, u\neq v, x\neq y, u\neq y, v\neq x) \\
&\left\langle \Psi^{(0)} | a^\dagger_{u\alpha} a_{v\alpha} a^\dagger_{x\beta} a_{y\beta} a^\dagger_{p\alpha} a_{q\alpha} a^\dagger_{r\alpha} a_{s\alpha} | \Psi^{(0)} \right\rangle (u\neq v, x\neq y, x\neq u || y\neq v)
\end{aligned} \tag{4}$$

As one could see, the first term can only contain 4 number operators to be non-zero. The second term can only contain 2 pair-double excitation operators. The third term can contain 2 number operators and one pair-double excitation operator.

Take the first term for example, there are only 4 possible cases for this term to be non-zero.

$$\begin{aligned}
&u=q, v=p, x=s, y=r \\
&u=s, v=p, x=q, y=r \\
&u=q, v=r, x=s, y=p \\
&u=s, v=r, x=q, y=p
\end{aligned} \tag{5}$$

For second term, the possible cases are

$$\begin{aligned}
&u=p, v=q, x=r, y=s \\
&u=r, v=q, x=p, y=s \\
&u=p, v=s, x=r, y=q \\
&u=r, v=q, x=p, y=s
\end{aligned} \tag{6}$$

Here we show how to build the 4RDM constructively. The problem is defined as the following.

$$\left\langle \Psi^{(0)} | a^\dagger_u a_v a^\dagger_x a_y a^\dagger_p a_q a^\dagger_r a_s | \Psi^{(0)} \right\rangle \tag{7}$$

where $u,v,x,y,p,q,r,s \in \{0,1,\cdots,2n-1\}$ indicating spin orbitals where n is the number of molecular orbitals. The indices u,v,x,y has the following additional constraints:

1. (u,v) and (x,y) must belongs to the same spin respectively
2. $u>x$, $v>y$
3. As generalized excitation term, u,v,x,y must not belong to same spin orbital, but they can be in the same molecular orbital of different spins
4. $a^\dagger_u a_v a^\dagger_x a_y$ must break the pair symmetry
5. $a^\dagger_u a_v a^\dagger_x a_y a^\dagger_p a_q a^\dagger_r a_s$ must conserve the pair symmetry

Since for each valid tuple of $(uvxy)$, there must be at least one valid $(pqrs)$ but not vise versa, it is more efficient to enumerate all valid $(uvxy)$ and derive its corresponding valid $(pqrs)$. All valid types of $(uvxy)$ are shown in Fig. 1 . For example, for (1) in Fig. 1, it means out of all molecular orbitals, choose four of them and assign the α spin part of the molecular orbital to $(uvxy)$. Notice, however, when enumerate all possible $(uvxy)$, it still needs to satisfy the additional condition that $x<u, y<v$.

For each of the above cases, we need to derive a matching $(pqrs)$ so that the combined eight indices sill preserve the symmetry. We showed all possible combinations of $(uvxy)$ and $(pqrs)$ in Fig. 2.

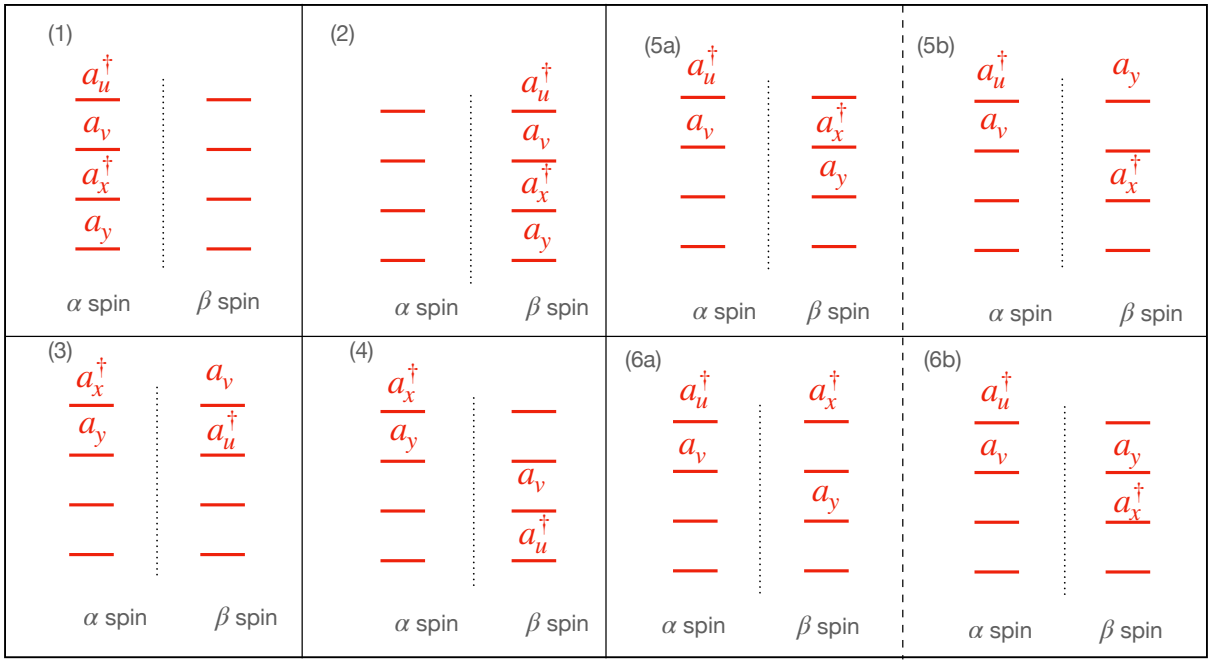

Supplementary Figure 1: All possible index combinations for $(uvxy)$ that breaks paired symmetry. The four levels corresponds to arbitrarily chosen four molecular orbitals among all possible molecular orbitals. The two bars on the same level corresponds to the two spin orbitals of the same molecular orbital. The spin types of $(uvxy)$ are described as the following. (1) $\alpha\alpha\alpha\alpha$ on different molecular orbitals. (2) $\beta\beta\beta\beta$ on different molecular orbitals. (3) $\alpha\alpha\beta\beta$ on two molecular orbitals. (4) $\alpha\alpha\beta\beta$ on four different molecular orbitals. (5) $\alpha\alpha\beta\beta$ on three molecular orbitals with (5a) annihilation-creation operators share the same molecular orbital or (5b) creation-annihilation operators share the same molecular orbital. (6) $\alpha\alpha\beta\beta$ on three molecular orbitals with (6a) two creation operators share the same molecular orbital or (6b) two annihilation operators share the same molecular orbital.

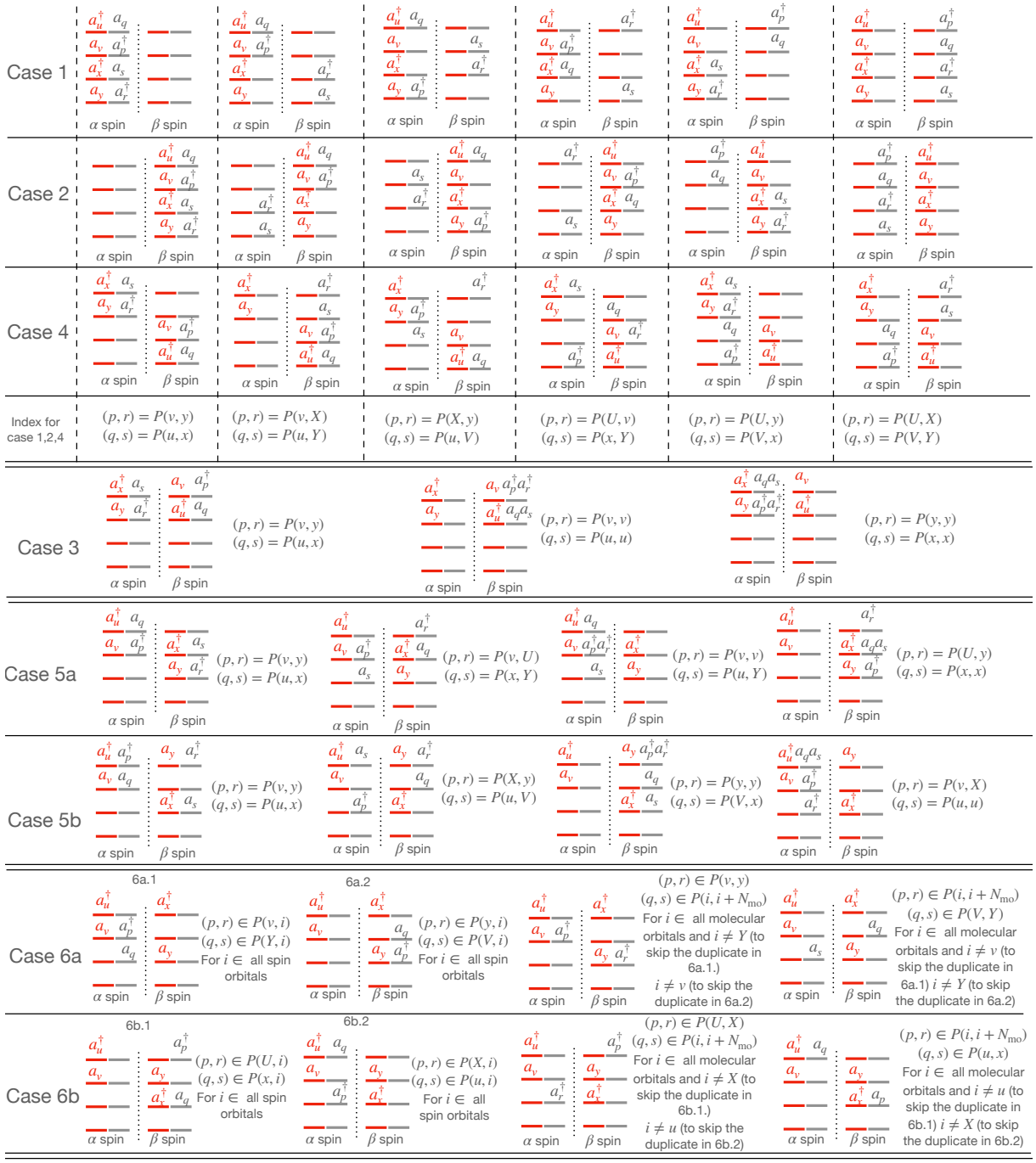

Supplementary Figure 2: The figure lists the rules to generate valid indices for $\left\langle \Psi^{(0)} | a_u^\dagger a_v a_x^\dagger a_y a_p^\dagger a_q a_r^\dagger a_s | \Psi^{(0)} \right\rangle$ for a given $a_u^\dagger a_v a_x^\dagger a_y$. All indices are spin orbital indices. $P(\cdot,\cdot)$ represents the permutation function to generate valid indices and is defined as $P(x,y) = \begin{cases} \{(x,y),(y,x)\} & \text{if } x \neq y \\ \{(x,x)\} & \text{if } x = y \end{cases}$. The capitalization of the letter indicates a index of opposite spin. For example, $U = u + N_{\text{mo}}$ if u is α spin and $U = u - N_{\text{mo}}$ if u is β spin, where N_{mo} is the number of molecular orbitals. For example, for all three cases (case 1, 2 and 4) in the first column, the (p,r) should be $P(v,y) = \{(v,y),(y,v)\}$ which means $p = v, r = y$ or $p = y, r = v$, while (q,s) should be $P(u,x) = \{(u,x),(x,y)\}$. So the valid operators are $a_u^\dagger a_v a_x^\dagger a_y a_v^\dagger a_u a_y^\dagger a_x$, $a_u^\dagger a_v a_x^\dagger a_y a_v^\dagger a_x a_y^\dagger a_u$, $a_u^\dagger a_v a_x^\dagger a_y a_y^\dagger a_u a_v^\dagger a_x$, $a_u^\dagger a_v a_x^\dagger a_y a_y^\dagger a_x a_v^\dagger a_u$.

Supplementary Note 3. EFFICIENT POST-PROCESSING

In this section we explain another major effort to improve the speed for evaluating the expectation value of second-quantized Hamiltonians that satisfy pair-symmetry. Since the second quantized operator O_J to be measured satisfies the pair symmetry, it can always be partitioned as

$$O_J = \prod_{jk} a_j^\dagger a_k \to (-1)^b \prod_{jk} a_{j\alpha}^\dagger a_{j\beta}^\dagger a_{k\alpha} a_{k\beta} \prod_l a_l^\dagger a_l \prod_m a_m a_m^\dagger \tag{8}$$

that is, paired excitation parts, and number operator parts. We then expand the fermionic operators with the following transformation

$$a_{j\alpha}^\dagger a_{j\beta}^\dagger = \frac{1}{2}(X_j - iY_j) \tag{9}$$

$$a_{j\alpha} a_{j\beta} = -\frac{1}{2}(X_j + iY_j) \tag{10}$$

$$a_l^\dagger a_l = \frac{1}{2}(I - Z_l) \tag{11}$$

$$a_l a_l^\dagger = \frac{1}{2}(I + Z_l) \tag{12}$$

and take only the real part. So each of the

$$O_J = \prod_{jk} a_j^\dagger a_k \mapsto \sum_j h_j \otimes_k \sigma_v^{(jk)} = \sum_j h_j P_j \tag{13}$$

where $\sigma_v \in \{I, X, Y, Z\}$ is one of the Pauli operators and P_j denotes a Pauli string. As a result, in order to obtain $\langle O_J \rangle$, we only needs to obtain $\langle P_j \rangle$.

Notice there will be many P_j that are duplicates from different O_J. To avoid duplicate measurement and post-processing, we first collect all unique P_j from all $\{O_J\}$ of interest to form a set $\{P_j\}$, obtain $\{\langle P_j \rangle\}$ and store it into a hash table (such as dictionary in Python). Then to recover the $\langle O_J \rangle$, we only need to retrieve the $\langle P_j \rangle$ from $\{\langle P_j \rangle\}$ and then sum them up with the weight h_j in each O_J. It is worth noting that, when measure the expectation value for $\{P_j\}$, we can measure several Paul strings simultaneously without the increase of the number of two-qubit gates as long as all Pauli strings to be measured simultaneously are mutually qubit-wise-commuting. In practice we use the qiskit qubit-wise-commuting function.

Supplementary Note 4. CONNECTION WITH MOLLER-PLESSET PERTURBATION THEORY

Our VQE-PT2 theory could be considered as a generalization of the traditional Moller-Plesset second order perturbation theory (MP2). In the case where $\left|\Psi^{(0)}\right\rangle$ is the Hartree-Fock state, the energy correction of VQE-PT2 becomes the energy correction of MP2, with contributions only from the broken-paired determinants. The G matrix becomes diagonal and its diagonal elements are the orbital energy differences in the denominator of MP2.

Supplementary Note 5. REGULARIZATION

The perturbation theory described in previous sections may run into numerical instability issues without regularization. The numerical instability arises from two reasons. First, if a broken-pair excitation in the wave function corrections excites an electron from (to) a nearly empty (occupied) orbital, then both G and Y would be small and their division in Equation **??** would be unstable. Second, since oo-upCCD includes orbital optimization effects, in bond breaking scenarios, the HOMO-LUMO gap closes as one stretches the bond, which also reduces the magnitude of G and leads to numerical instability.

In order to tackle this problem, we take the same approach of the orbital optimized Møller-Plesset second order perturbation theory (ooMP2)[7, 8] and add a regularization to the amplitude, which becomes

$$t_p = -\frac{Y_p}{G_{pp}}(1 - e^{-\sigma G_{pp}}) \tag{14}$$

in which we introduce an empirical parameter σ that controls the strength of the regularization.

As one could see, if $G = 0$, then the regularized t_p also becomes zero and it no longer contributes to the wave function. In the regularized ooMP2, σ is obtained by fitting to a known database, and the optimal σ is found to be 1.5. In our case, we use a much larger σ, which is chosen to be 28.

This σ is chosen so that terms with $G_{pp} < 1 \times 10^{-4}$ is completely damped away to avoid numerical instabilities. One of the main reason that it is much larger than the regularization parameter in regularized ooMP2 is because the numerical instability issue in VQE-PT2 is much less severe that in ooMP2, as a large portion of correlation energy is treated variationally by the VQE ansatz in VQE-PT2, and the perturbation theory only needs to take into account of the broken pair configurations. This allows us to use a larger σ, which does not damp away correlation energies and only remove the numerical instability when G_{pp} approaches zero, while it only damps little correlation energy away when G is far away from zero. Admittedly, finding σ by fitting to a data set is a more accurate path for finding σ. However, optimal selection of σ is beyond the scope of the present study, and we hope to investigate it in future studies.

[1] Qiskit contributors. Qiskit: An Open-Source Framework for Quantum Computing (2023).
[2] Sun, Q. *et al.* PySCF: the Python-Based Simulations of Chemistry Framework. *Wiley Interdiscip. Rev. Comput. Mol. Sci.* **8** (2018).
[3] Rhee, Y. M. & Kim, M. S. Dynamic Isotope Effect on the Product Energy Partitioning in $CH_2OH^{\rightarrow}CHO^{+}$+$H_2$. *J. Chem. Phys.* **109**, 5363 (1998).
[4] Henkelman, G., Uberuaga, B. P. & Jónsson, H. A Climbing Image Nudged Elastic Band Method for Finding Saddle Points and Minimum Energy Paths. *J. Chem. Phys.* **113**, 9901–9904 (2000).
[5] Henkelman, G. & Jónsson, H. Improved Tangent Estimate in the Nudged Elastic Band Method for Finding Minimum Energy Paths and Saddle Points. *J. Chem. Phys.* **113**, 9978–9985 (2000).
[6] Sheppard, D., Terrell, R. & Henkelman, G. Optimization Methods for Finding Minimum Energy Paths. *J. Chem. Phys.* **128**, 134106 (2008).
[7] Lee, J. & Head-Gordon, M. Regularized Orbtital-Optimized Second-Order Møller-Plesset Perturbation Theory: A Reliable Fifth-Order-Scaling Electron Correlation Model with Orbital Energy Dependent Regularizers. *J. Chem. Theory Comput.* **14(10)**, 5203–5219 (2018).
[8] Shee, J., Loipersberger, M., Rettig, A., Lee, J. & Head-Gordon, M. Regularized Second-Order Møller–Plesset Theory: A More Accurate Alternative to Conventional MP2 for Noncovalent Interactions and Transition Metal Thermochemistry for the Same Computational Cost. *J. Chem. Theory Comput.* **12(50)**, 12084–12097 (2021).